Is the 'shark–skin effect' in films over undulated substrates possible? Resistance reduction in creeping films

M Scholle *and* ***N Aksel***
Department of Applied Mechanics and Fluid Dynamics, University of Bayreuth, D-95440 Bayreuth, Germany

If a body in a flow is provided with small ridges aligned in the local flow direction, a remarkable drag reduction can be reached under turbulent flow conditions. This surprising phenomenon is called 'shark skin effect'. Since for coating processes often low Reynolds numbers are relevant, we examine the possibility of a resistance reduction due to a rippled surface topography in Stokes flow. We especially analyse the influence of wall riblets perpendicular to the flow direction on the mean transport velocity in gravity–driven creeping film flows following the idea that eddies generated in the valleys of the riblets act like 'fluid roller bearings' and hence can reduce drag. Parameter studies with varying flow rate, bottom amplitude and bottom shape are presented. For the given bottom shapes the maximum enhancement of transport velocity is found by optimizing the film thickness.

1 Introduction

It is yet controversely discussed that the dermal surface morphology of sharks is in order to improve the sharks' swimming performance [1]. Nevertheless, it is widely accepted that for bodies in turbulent flows a reduction of skin friction by some percent can be reached if the surface of the body is provided with small ridges aligned in the local flow direction [2]. This rather counter–intuitional phenomenon occurs in turbulent flows. Here, we address a fundamental question: Is drag reduction possible if inertia is absent, e.g. in creeping flows?

In the present article we investigate in film flows over a periodic topography. Film flows occur in many technical processes as well as in nature. In the large field of coating techniques, especially where thin liquid films are forced to spread over solid substrates, they are of a great importance. Flows of this type are found e.g. in the manufacturing of electronic devices. We especially consider a steady, gravity–driven film flow of an incompressible Newtonian fluid on an inclined plane. The bottom of the inclined plane is provided with periodic corrugations according to Figure 1.

Our investigations are motivated by the following idea: if the bottom is provided with riblets aligned perpendicular to the flow direction, kinematically induced eddies can be created even in creeping flows where inertia is absent. These eddies are expected to act like 'fluid roller bearings' and therefore to induce a positive effect on the mean transport velocity in the film.

2 Mathematical formulation

2.1 Basic assumptions, scalings and method of solution

We assume that the flow is steady, two–dimensional, creeping and that the film is thick enough such that the surface curvature can be neglected [3]. According to Figure 1, the mean film thickness is denoted by H, the periodic length by λ and the mean inclination angle by α. Cartesian coordinate system is used with the x–axis placed at the mean level of the bottom contour, the y–axis in line with the ridges and the z–axis normal to the mean level of the bottom.

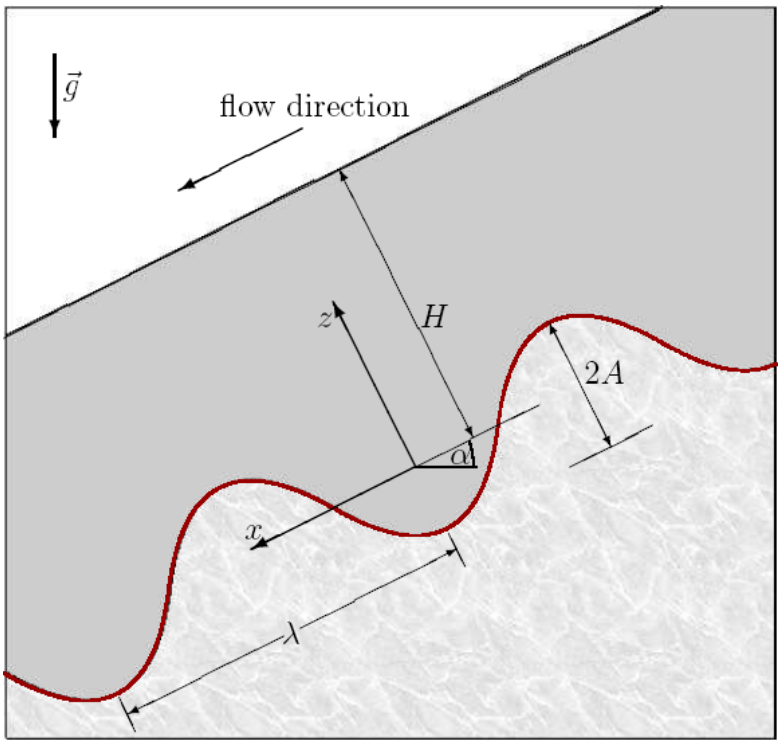

Figure 1: Sketch of the flow geometry.

As characteristic length $\lambda/2\pi$ is used for the scaling of all lengths in both directions. By $U := \rho g \lambda^2 \sin\alpha / \left(8\pi^2 \eta\right)$ both velocity components are scaled, by the characteristic shear stress $2\pi\eta U/\lambda$ the pressure is scaled. Due to the vanishing surface curvature and above scaling the dimensionless mean geometrical film thickness $h = 2\pi H/\lambda$ and the bottom topography $b(x)$ are the only parameters which enter the problem.

The basic equations are the continuity equation and Stokes' equations, supplemented by the no–slip condition at the bottom and the kinematic and dynamic boundary conditions at the surface. Their solution is calculated by a semi–analytical approach based on complex variable method, which allows for a reduction of the problem to the solving of an algebraic set of equations. This method and the solving procedure is described in detail in the articles [3,4].

2.2 Bottom topography

For the modelling of wall roughness Panton [5] suggests a 'brush model', i.e. an infinite array of equidistant narrow peaks. Therefore, we choose the topography $b(x)$ among a class of functions with similar properties. We especially consider trigonometric polynomials

$$b_N(x) = \sum_{n=1}^{N} B_n \cos nx \qquad (1)$$

with the N coefficients B_n uniquely determined implicitly by the N conditions

$$\begin{aligned} b_N(\pi) - b_N(0) &= 2a \\ \left.\frac{\mathrm{d}^{2k} b_N}{\mathrm{d}\, x^{2k}}\right|_{x=0} &= 0 \end{aligned} \qquad (2)$$

where $k = 1, \cdots, N-1$. Obviously, the first equation in (2) is a normalisation condition for the non–dimensional amplitude $a := 2\pi A/\lambda$ of the topography. By means of the second condition

in (2) all derivatives of $b_N(x)$ in $x=0$ up to the order $2N-2$ vanish. The resulting shapes, which are shown in Figure 2 for $N=1$, 3 and 10 are equidistant narrow peaks at $x=\pm\pi$ with nearly planar regions between the peaks. These shapes are subsequently called peak arrays of order N.

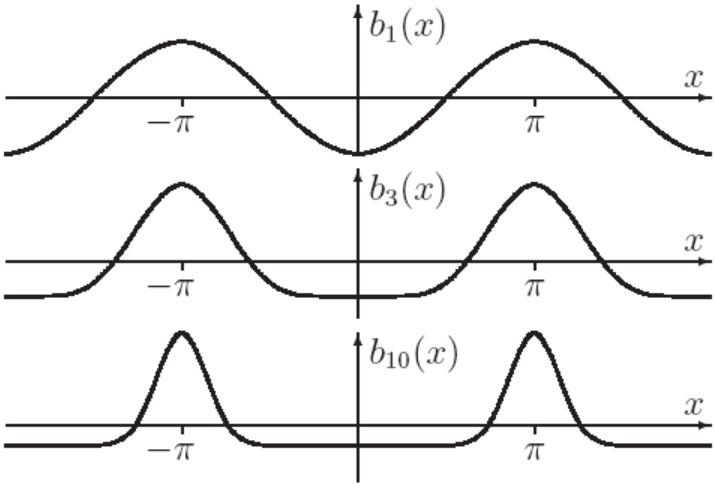

Figure 2: Three different bottom shapes.

By increasing the order N, the peaks becomes more and more narrow. These shapes provide good approximations for the idealised array of brush–like narrow peaks.

2.2 Mean transport velocity

We define the mean transport velocity as

$$u_t = \frac{\dot{V}}{h_t} \tag{3}$$

with the two–dimensional flow rate $\dot{V}$ and the mean transport thickness h_t. The latter one has to be understood as mean thickness of the cross section of the flow which contributes to the material transport, i.e. the film above the separation areas. If the separatrix of the primary eddy is given as $z=s(x)$, $-x_0 \le x \le x_0$ with x_0 denoting the x–positions of the triple points, the mean transport thickness results in

$$h_t = h - \frac{1}{2\pi}\int_{-x_0}^{x_0}\left[s(x)-b(x)\right]\mathrm{d}x \tag{4}$$

Furthermore, by

$$h_0 = \sqrt[3]{\frac{3}{2}\dot{V}} \tag{5}$$

the reference thickness of a film flow on a plane bottom with the same flow rate as the flow over the topography is defined. The three quantities h_0, h and h_t are illustrated in Figure 3. Thus, for a fixed flow rate $\dot{V}$, the comparison of the mean transport thickness h_t with the reference thickness h_0 delivers an adequate measure for enhancement or reduction of the mean transport velocity in the film: In case of $h_t > h_0$, the mean transport velocity is reduced, whereas $h_t < h_0$ indicates enhancement of u_t.

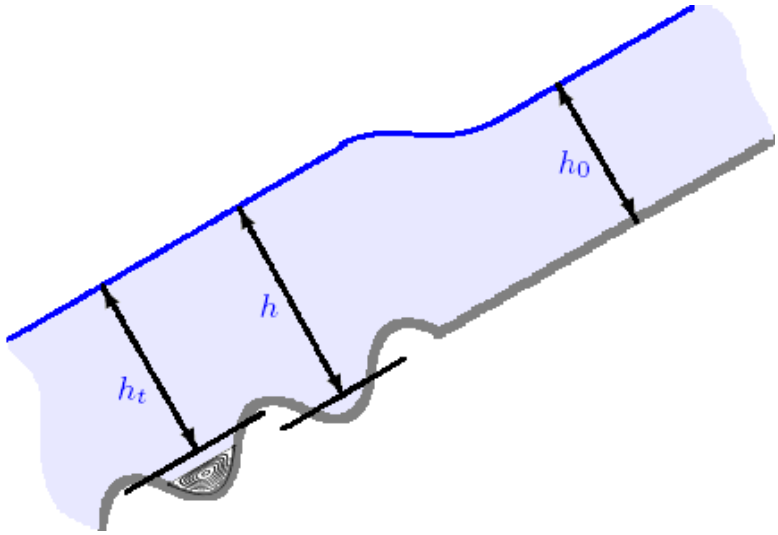

Figure 3: Mean transport, mean geometrical and reference film thickness.

3 Results

3.1 Streamlines and eddy creation

Streamline patterns have been calculated for various shapes, amplitudes and film heights. For small amplitudes the streamlines follow the bottom contour, whereas flow separation is observed if the amplitude exceeds a critical limit. As representative examples in Figure 4 the streamlines in the vicinity of the bottom are presented for the shape b_{10} with two different amplitudes, namely $a = 0.34\pi$ and $a = 1.0\pi$.

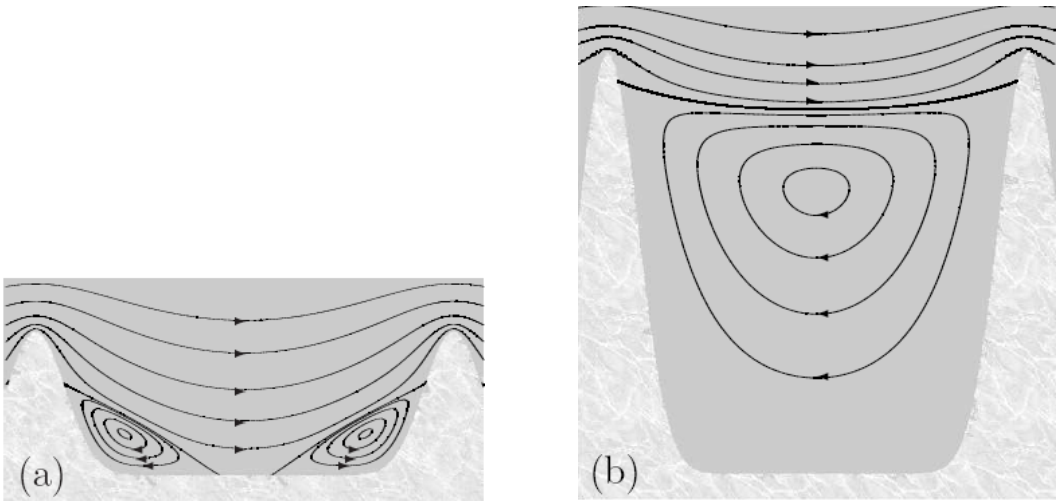

Figure 4: Near--bottom streamlines of film flows over the topography b_{10} with non–dimensional amplitude (a) $a = 0.34\pi$ and (b) $a = 1.0\pi$.

The reference film thickness is $h_0 = 3\pi$ in both cases. The critical amplitude for the primary flow separation is $a \approx 0.214\pi$. Thus, in Figure 4a flow separation is already apparent: A pair of eddies has been created at the positions of maximum curvature. With increasing amplitude the eddies are growing, which leads to the merging of the two eddies to a single one. Such a case with a large single eddy which covers the major part of the region between two neighbouring peaks is shown in Figure 4b. In this example we especially see a slightly curved separatrix passing nearly from tip to tip. This feeds the hope of a probable resistance reduction, since the eddies are supposed to act like 'fluid roller bearings'. By increasing the amplitude further, a

secondary pair of eddies is created at the critical amplitude $a \approx 1.212\pi$ for secondary flow separation.

3.2 Mean transport velocity

In Figure 5 the relative film elevation $(h_t - h_0)/h_0$ is plotted versus the amplitude a for the three different bottom contours b_1, b_3 and b_{10}. This parameter study has been carried out with a fixed flow rate of $\dot{V} = 18\pi^3$, corresponding to a reference thickness of $h_0 = 3\pi$. Additionally, the onset of primary and further flow separation is indicated in the diagram. From the beginning up to an amplitude of about $\pi/3$, the film elevation is monotonously increasing for all three different shapes, which indicates a reduction of the mean transport velocity due to the bottom corrugations. Note, that within this parameter regime no positive effect can be expected since no eddies are present. However, the curves reach maxima slightly after the primary eddy generation and pass then into a monotonous decrease due to reduction of friction by the eddies. Obviously, both the height of the maximum as well as the decrease after the eddy generation are more pronounced for bottom shapes with sharper peaks.

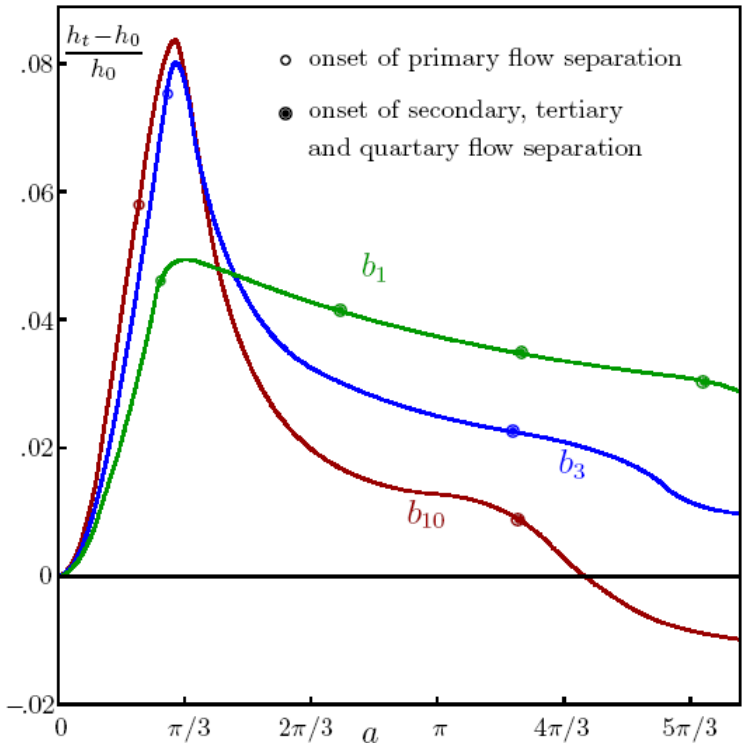

Figure 5: Relative film elevation vs. amplitude of flows over different shapes.

For the curve associated to the bottom b_{10} the film elevation becomes negative for high amplitudes, i.e. the mean transport velocity exceeds the corresponding mean transport velocity of the flow over a plane bottom. At the highest amplitude considered in our calculations, $a = 1.8\pi$, this enhancement of the mean transport velocity reaches 0.88%.

The increase of the mean transport velocity indicates an improved mass transport in the volume. In contrast to this, our calculations delivered no significant changes in the surface velocity. Hence, the influence of bottom corrugations and eddies on the flow is restricted to the near–bottom region of the film. Thus, it should be expected that the relative enhancement of the mean transport velocity is larger in thinner films. On the other hand, the eddies are shrinking when the film thickness is decreased, which leads to a smaller enhancement of the mean transport velocity. In very thin films the eddies can be even completely suppressed, see [3], whereas in

very thick films the size of the eddies reaches an asymptotic value and therefore the relative effect tends with $\sim h_0^{-1}$ to zero for increasing h_0. Hence, for a given bottom topography an optimum film thickness exists. Besides, a stronger drag reduction is found for sharper peaks. Focusing on the peak array of order 10 for fixed bottom amplitude $a = 1.6\pi$ and varying the reference film thickness, we found according to Figure 6 the optimum relative film elevation and therefore a maximum enhancement of the mean transport velocity of 1% at a reference film thickness of $h_0 = 3.75\pi$.

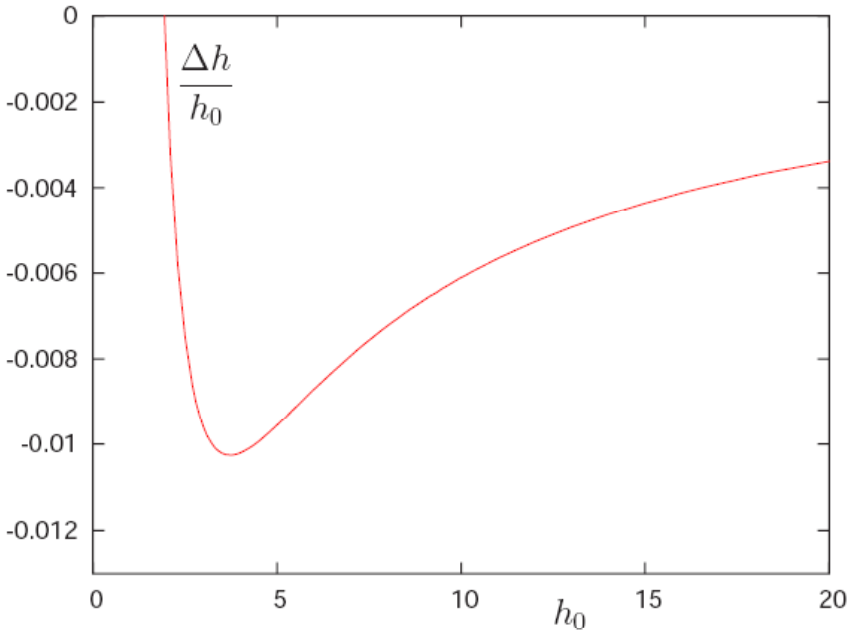

Figure 6: Relative film elevation vs. reference film thickness for the peak array of order 10 with non–dimensional amplitude $a = 1.6\pi$.

4 Conclusions

The parameter studies on the three different topographies b_1, b_3 and b_{10} revealed a noticeable effect of the bottom on the material transport in a creeping film flow: For the shapes b_1 and b_3 we found a decrease of the mean transport velocity compared to the flow over a plane bottom, whereas for the shape b_{10} with the sharpest peaks an increase of the mean transport velocity becomes apparent at sufficiently high amplitude. Thus, a comparison to the 'shark skin effect', which has been successfully applied to ships and airplanes for drag reduction, is near at hand. The present effect, however, is essentially different from the popular shark skin effect: The increase of the mean transport velocity has been calculated for creeping flows, whereas the shark skin effect occurs in turbulent flow at Reynolds numbers $10^4 - 10^6$. Furthermore, the rippled structures of the shark skin are directed longitudinal to the flow, not transversal as it is the case here. The explanation for these differences are the different mechanisms behind the two effects: In case of the classical shark skin effect, the control of the streamwise eddies in the turbulent flow gives rise to drag reduction [2], whereas in case of creeping films the rippled bottom topography enforce the creation of eddies which act on the flow like a kind of fluid roller bearing. Nevertheless, a common feature of the shark skin effect and the effect observed in the present paper is the reduction of resistance in the flow by means of rippled wall structures.

On the other hand, the eddies have a vanishingly small effect on the surface velocity of the film, compared to the influence on the mean transport velocity. This shows that the drag reduction effect is located in the near–bottom region.

A parameter study on the film thickness revealed the maximum enhancement of the mean transport velocity of 1% . It is found at an optimum film thickness of $h_0 = 3.75\pi$. Although an improvement of 1% seems to be a small effect, the benefit of a rippled structure can be worthwile in long term processes. It is an open question up to which extend the value of 1% can be improved by varying the bottom shape.

5 References

1. Vogel, S., 1996, Life in Moving Fluids, Princeton University Press, 153–154
2. Koeltzsch, K., Dinkelacker, A. and Grundmann, R., 2002, Flow over convergent and divergent wall riblets, *Exp. Fluids,* **33,** 346–350
3. Scholle, M. and Aksel, N., 2004, Creeping films with vortices over strongly undulated bottoms, *Acta. Mech.*, **168**, 167-193
4. Scholle, M. and Aksel, N., 2004, Drag reduction and improvement of material transport in creeping films, *Arch. Appl. Mech.* (accepted for publication)
5. Panton, R. L., 1996, Incompressible Flow, Wiley Interscience